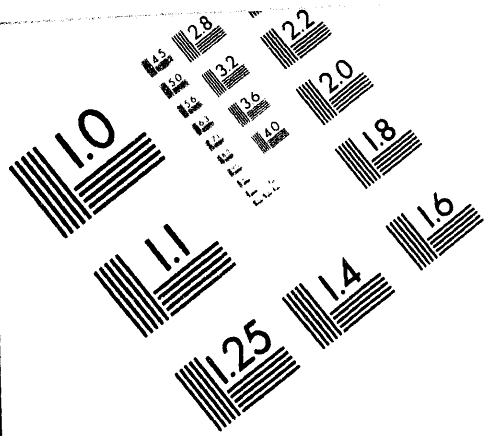

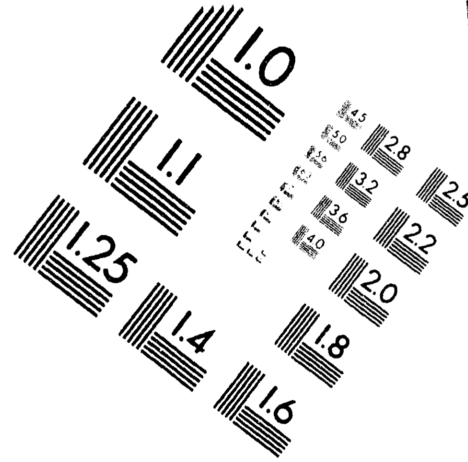

AIIM

Association for Information and Image Management

1100 Wayne Avenue, Suite 1100
Silver Spring, Maryland 20910

301/587-8202

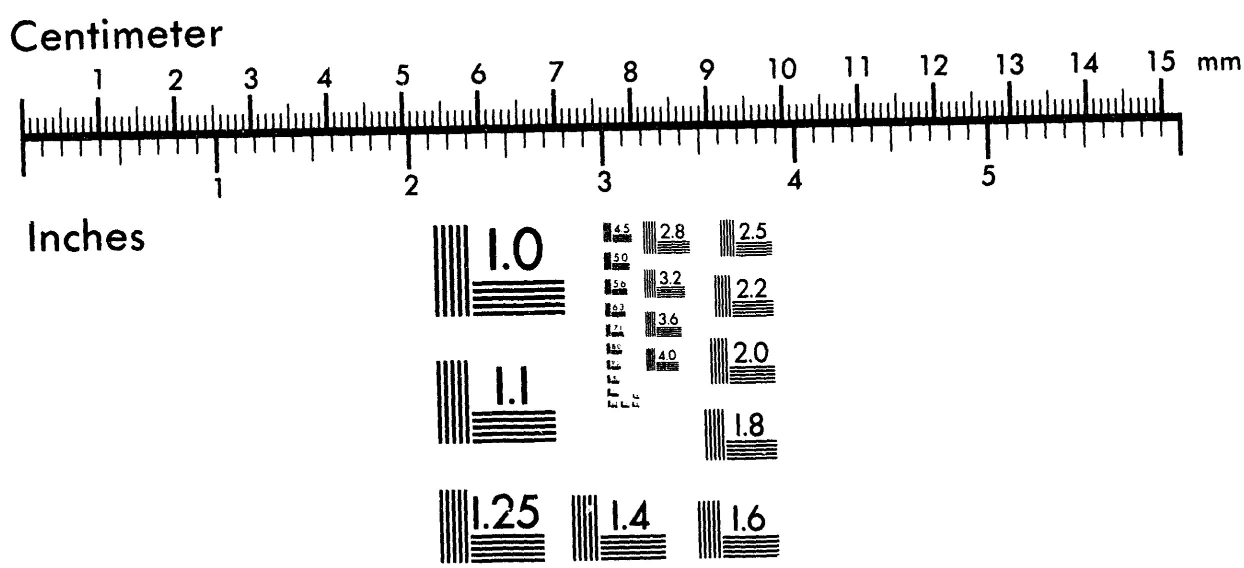

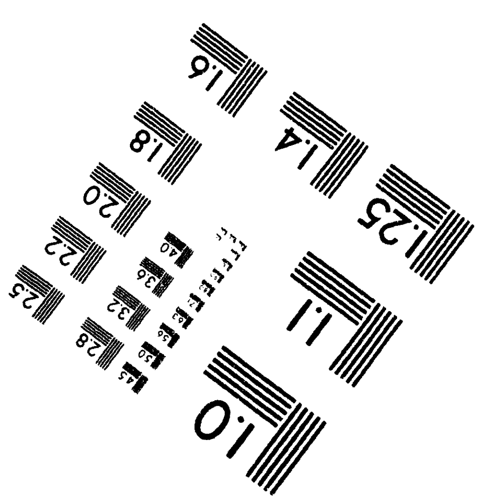

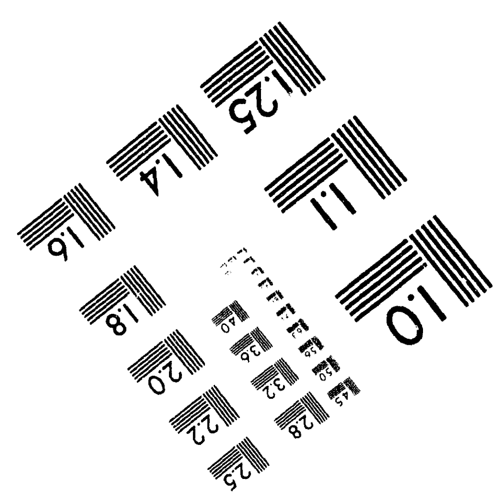

1 of 1

Thermo-Mechanical Analysis of the White-Beam Slits for an Undulator Beamline at the Advanced Photon Source

H. L. Thomas Nian, D. Shu, and Tuncer M. Kuzay

Argonne National Laboratory

9700 South Cass Ave.

Argonne, IL 60439

Abstract

A set of precision horizontal and vertical white-beam slits has been designed for an undulator beamline at the Advanced Photon Source. Due to the powerful x-ray heat flux emitted by the undulator, it is difficult to control the thermal distortion within the desired range of 1-2 microns. We analyzed many conceptual designs in an attempt to minimize the thermal distortion of the slits. Even with 1-mm-thick, low-Z material (graphite) coated on the heating surface of a traditional slit, the maximum thermal distortion is over 25 microns. A three-piece slit was then designed to satisfy the requirements. It consists of one large block, two tungsten knife edges, and an OFHC cooling tube (filled with copper mesh) brazed inside the large block. The thermal distortion at the knife edges of this three-piece slit has a relative displacement of less than 2 microns.

1 Introduction

A set of precision horizontal and vertical white-beam slits has been designed [1] for an undulator beamline at the Advanced Photon Source (APS). The slit, a knife-edge-type precision device, is required to have very small thermal distortion during operation with beam. The traditional slit consists of a large block and an OFHC cooling channel inside the block. Some users require that the thermal distortion be as small as about 1-2 microns at the knife edge. Due to the powerful x-ray heat flux coming from APS Undulator A [2], it is an exceedingly difficult problem to reduce the thermal distortion to less than 2 microns.

Dealing with the heat flux from Undulator A is an engineering challenge. At normal incidence, the peak power is about $175\frac{W}{mm^2}$ at 27.5 m, with a total power of 3.8 kW. The Gaussian deviation is about 1.22 mm, and the parabolic deviation is about 3.8 mm. The footprint of the x-ray beam is very small, which induces a very high thermal stress. A FORTRAN code allows the element (in the ANSYS finite element code used) subjected to the x-ray beam to get the power distribution automatically at its coordinate position.

Enhanced heat transfer technology [3] was used to increase the convective heat transfer coefficient with water from 1 $\frac{W}{cm^2 \cdot {}^\circ C}$ to about 3 $\frac{W}{cm^2 \cdot {}^\circ C}$ for the OFHC tube. However, we assumed a convective heat transfer coefficient of 2$\frac{W}{cm^2 \cdot {}^\circ C}$ in conservative calculations.

2 Material Considerations

It is very important that the slit body be made of a material having a very low thermal expansion coefficient and a high thermal conductivity. Both TZM (vacuum arc-cast molybdenum-0.5% titanium-0.1% zirconium alloy) and tungsten alloy (HD18) [4] were considered for the block material. OFHC is the material for the cooling tube. During operation, both the HD18 and TZM will reach temperature levels of about 400°C. Therefore, the material properties at such elevated temperatures were considered in the analysis. Table 1 shows the properties of the materials considered for the slit.

Table 1. Properties of the Materials Considered for the Slit

	Room Temperature			400°C	
Properties	TZM	HD18	OFHC	TZM	HD18
Conductivity K $\frac{W}{cm\ {}^\circ K}$	1.45	1.65	3.95	1.3	1.35
Young's Modulus E MPa	3.15×10^5	3.65×10^5	1.19×10^5	3.0×10^5	3.1×10^5
Thermal Exp. Coef. α $\frac{1}{{}^\circ C}$	5.4×10^{-6}	4.5×10^{-6}	17.7×10^{-6}	5.6×10^{-6}	4.6×10^{-6}
Poisson Ratio ν	0.293	0.28	0.307	.361	.28
Yield Strength σ_y	1000	580	300	800	380
Ultimate Strength σ_u MPa	1000+	1500+	350	1000+	1500+

When the temperature rises from room temperature to about 400°C, the yield strength of HD18 will drop from 580 MPa to 380 MPa. Therefore, we decided to use TZM as the material for the large block because its yield strength (test at 0.05 inch per inch per minute, vacuum 10^{-5} mm Hg) is above 1000 MPa at room temperature and is about 700 MPa at 500°C. (Without the vacuum test condition, the TZM also performs well; for a 0.06-inch stress-relieved sheet, the yield strength is above 1000 MPa at room temperature and is about 690 MPa from $400°C$ to $650°C$.)

3 Design Progression

We analyzed many large block conceptual designs in order to

1. reduce the maximum temperature of the large block to under $400°C$ if tungsten is used,
2. reduce the maximum thermal distortion to the required 1-2 microns,
3. reduce the interfacial stress between the big block and the OFHC cooling tube,
4. reduce the localized stress concentration at the support area.

The slit design progressed in several stages due to severe distortion problems under the predicted heat load. The analysis proves that a single piece of large block will always have a thermal distortion of about 90 microns (when subjected to Undulator A heat flux) with the best possible boundary conditions for cooling and supporting. Even with a 1-mm-thick, low-Z material (graphite) coated on the heating surface $\diamond ADEF$ of the large block (see Fig. 1), the maximum thermal distortion is still over 25 microns. In order to reduce the thermal distortion to 2 microns, a three-piece slit was designed [1] that consists of one large block (as shown in Fig. 1), two tungsten knife-edge small blocks (as shown in Fig. 2), and an OFHC cooling tube brazed inside the large block. The major function of the large block is to act as an absorber that will take most of the heat flux. This results in a maximum deflection of about 100 microns in the large block (final design). The thermal distortion at the knife edges of this three-piece slit has a relative displacement of less than 2 microns.

Figure 1 depicts the large slit block geometry of the final design. It is about 300 × 26 × 52 mm (x, y, and z coordinates, respectively). Due to the limited space, the grazing incidence angle is fixed at 2.5° on both $\diamond ADEF$ and $\diamond ABGH$ surfaces (as shown in Fig. 1).

The critical surfaces [1] shown in Fig. 1 are :

1. $\triangle$ ACD, which causes a clear cut of the x-ray beam in the horizontal plane. U_y (displacement in y-axis) is the only important displacement at this surface.
2. $\triangle$ ABC, which creates a clear cut of the x-ray beam in the vertical plane of the x-ray beam. U_z is the only important displacement at this surface.

Both $\triangle ACD$ and $\triangle ABC$ will never be hit by the x-ray beam [1]. When the beam hits $\diamond ADEF$ (in Fig. 1), the vertical beam is stretched out along the x-axis. When the beam hits $\diamond ABGH$ (in Fig. 1), the horizontal beam is again stretched out along the x-axis. However, the beam-spreading length in the x direction on $\diamond ABGH$ is two times more than that on $\diamond ADEF$, which implies that the temperature and resulting thermal stress on $\diamond ADEF$ will be about twice those on $\diamond ABGH$.

A closed form solution (see [5]) is used for the design optimization. The heat equation for a thermal plate (as shown in Fig. 3) subjected to a Gaussian-distributed heat flux is

$$\frac{\partial^2 T}{\partial x^2} + \frac{\partial^2 T}{\partial y^2} = 0. \tag{1}$$

The boundary conditions are

$$\begin{aligned}
-k\frac{\partial T}{\partial y}(x,0) &= q_o exp\left(-\frac{x^2}{r_o^2}\right) \quad 0 \le x \le a. \\
-k\frac{\partial T}{\partial y}(x,0) &= 0 \qquad\qquad a < x \le b \\
-k\frac{\partial T}{\partial y}(x,t) &= h_c(T - T_\infty) \\
\frac{\partial T}{\partial x}(0,y) &= \frac{\partial T}{\partial x}(b,y) = 0.
\end{aligned} \tag{2}$$

The solutions give

$$\theta = C_o\left[\eta - 1 - \frac{1}{Bi}\right] + \sum_{m=1}^{\infty} C_m e^{-\lambda_m \eta}\cos(\lambda_m \xi)\left[1 + \frac{\lambda_m - Bi}{\lambda_m + Bi}e^{2\lambda_m(\eta-1)}\right], \tag{3}$$

where

T:	Temperature (°C)
k:	Thermal conductivity (W/m·°C)
XYZ:	Fixed coordinate
q:	Heat flux (W/m^2)
t:	Thickness of plate (m)
h:	Convective heat transfer coefficient ($W/m^2 \cdot$ °C)
T_∞:	Ambient temperature (assumed to be 24°C)
b:	Width of the plate (m)
a:	Width where q is applied to the large block (m)
r_o	Standard deviation (m),

and

$$\begin{aligned}
\alpha &= \frac{a}{t}, \quad \beta = \frac{b}{t}, \quad \xi = \frac{x}{t} \\
\eta &= \frac{y}{t}, \quad \theta = \frac{k(T - T_\infty)}{qt}, \quad Bi = \frac{h_c t}{k},
\end{aligned} \tag{4}$$

$$C_o = -\frac{r\sqrt{\pi}}{2\alpha} erf\left(\frac{\alpha}{r}\right); \tag{5}$$

$erf(...)$ is known to be the *error function*, and

$$C_m = -\frac{\sqrt{\pi}\ r\ exp\left(-\frac{r^2\lambda_m^2}{4}\right) Re\left[erf\left(\frac{2\alpha + ir^2\lambda_m}{2r}\right)\right]}{\lambda_m\alpha\left(-1+e^{-2\lambda_m}\frac{\lambda_m - Bi}{\lambda_m + Bi}\right)}, \qquad \lambda_m = \frac{m\pi}{\beta}, \quad m \in N. \tag{6}$$

The analysis indicates that, while the tube I.D. (inside diameter) of the large block is fixed at 12.7 mm and h=2$\frac{W}{cm^2 \cdot {}^\circ C}$, the lowest surface temperature is obtained if the wall thickness (the distance between the heating surface and the inside wall of the tube) equals 3-4 mm as shown in Fig. 4. The average wall thickness of the design is about 14.5 mm (11 mm at $\overline{AF}$, 18 mm at $\overline{ED}$ as shown in Fig. 1). A decrease in the value of h from 2$\frac{W}{cm^2 \cdot {}^\circ C}$to 1$\frac{W}{cm^2 \cdot {}^\circ C}$ will increase the maximum temperature from 410°C to 500°C. Increases in the I.D. also help to decrease the maximum temperature. Also, while the average wall thickness is fixed at 14.5 mm and h=2$\frac{W}{cm^2 \cdot {}^\circ C}$, increasing the tube I.D. from 5 mm to 10 mm will decrease the maximum temperature from 636°C to 450°C. It was suggested that the cooling channel be designed so that it remains parallel to the heating surface in order to keep the wall thickness at a constant 5 to 6 mm. However, this idea compounds the design difficulty so we stayed with the design as shown in Fig. 1.

The most significant design changes after optimization were:

1. **The outer diameter of the cooling channel was increased from 16 mm to 19 mm as shown in Fig. 1.**
2. **The cooling channel is closer to the heating surface, from 11 mm at $\overline{AF}$ to 18 mm at $\overline{ED}$ (as shown in Fig. 1), which is about an average of 2 mm less than in the original design.**

4 Results and Discussion

4.1 Large Block

The worst possible case for the temperature field is when the beam center hits 3 mm away from $\overline{AD}$ and 15 mm away from $\overline{ED}$ on $\Diamond ADEF$ (in Fig. 1). The worst possible case for both thermal distortion and the stress field is when the beam center hits around $\overline{AF}$ and 3 mm from $\overline{AD}$ on $\Diamond ADEF$ (as shown in Fig.

1). Because the maximum temperature is not a concern, we will focus on the worst case for the thermal distortion and stress field in the following discussions.

Figure 5 shows the temperature contour of the large block. Figure 6 shows the displacement (U_z) contour. The calculated results for the original and final designs are shown in Table 2.

Table 2. Calculated Results from ANSYS Finite Element Code for the L5 Slit

	Final Design (Tube O.D.=19-mm)			Early Design (Tube O.D.=16-mm)		
h($\frac{W}{cm^2\,°C}$)	1	2	3	1	2	3
Max. Temp on Slit Surface (°C)	471	424	406	600	540	520
Max. Eff. Stress on Surface (MPa)	384	374	372	380	374	370
Max. Temp at Interface (°C)	191	138	120	180	150	140
Max. Eff. Stress at Interface (MPa)	273	177	141	300	230	165
Max. Deflection U_y at △ ACD ($micron$)	20	16	15	25	20	20
Max. Deflection U_z at △ ABC ($micron$)	110	90	85	150	125	115

The stress component σ_x on $\Diamond ADEF$ is much larger than the other two components, σ_y and σ_z, because the thermal gradient is much larger in that direction (the beam-spreading direction). The maximum displacement of the whole structure is in the x direction (U_x), if free expansion is allowed. The slit design [1] allows the large block to expand freely along the x-axis; the minimum σ_x on $\Diamond ADEF$ is about 410 MPa (compressive stress). If the expansion along the x-axis is totally constrained, the minimum σ_x becomes about 460 Mpa (compressive stress). Because the displacement component U_x in the large block is not a concern, to allow it to expand freely in the longitudinal (x) direction will reduce the stress component σ_x by 12%; also, the effective stress will be reduced by about 10%. The other two displacement components, U_y and U_z, are relatively small at the pin-hole area as shown in Fig. 1. The thermal stress is small even when the block is fully constrained in both the y and z directions around the pin-hole area.

For the final design, increasing h from $1\frac{W}{cm^2 \cdot °C}$ to $2\frac{W}{cm^2 \cdot °C}$ will help to:

1. decrease the displacement component U_z from 110 microns to 90 microns,
2. decrease the maximum interfacial stress (between the large block and the OFHC cooling tube) from 273 MPa to 177 MPa, which helps the OFHC remain in elastic deformation, and
3. decrease the maximum temperature at the bonding surface from 191°C to 138°C, which will keep the OFHC from approaching the annealing temperature (175°C).

Increasing the depth in the z direction will increase I_y. This helps to reduce U_z on the $\triangle$ ABC, but will decrease the natural frequency from the vibration point of view. The height in the original design was 36 mm compared to 52 mm in the final design (as shown in Fig. 1). To increase the height another 10 mm to 62 mm will help to reduce U_z at $\triangle$ ABC by 8 microns with the same boundary conditions.

When the x-ray beam hits both $\diamond ADEF$ and $\diamond ABGH$, the power deposited on them is complicated. Figure 7 (model for the original design) shows the temperature contour of such a case. It is easy to see that the x-ray beam extends much longer on $\diamond ABGH$ than on $\diamond ADEF$. When more x-ray beam deposits on $\diamond ABGH$ and less on $\diamond ADEF$, the resulting temperature, stress, and distortion are less severe. Besides, more x-rays will pass through $\angle DCB$ instead of being desposited on the large block.

4.2 Knife Edge

Only HD 18 was considered as the material for the two knife-edge slits. The two knife edges slits are V1, which defines the vertical beam, and H1, which defines the horizontal beam. Edge V1 is sitting on $\diamond EDMN$ in Fig. 1. Edge H1 is sitting behind the V1. Both V1 and H1 have very small surface areas, which will be subjected to the normal incident x-ray radiation from Undulator A. The small surface area of H1 is about 50 micron $\times$ 71 mm, located from $\overline{CD}$ to 50 microns in the positive y direction of $\overline{CD}$ (in Fig. 1). The dimension in the z direction is the same as $\overline{CD}$ at 71 mm. The small surface area of V1 is about 100 micron $\times$ 65 mm, located from $\overline{CB}$ to 100 microns in the positive z direction of $\overline{CB}$ in Fig. 1. The dimension in the y direction is the same as $\overline{CB}$ at 65 mm.

Edge V1 will absorb 114 W in the worst case. Edge H1 will be subjected to about 50 W in the worst case. V1 and H1 do not have a cooling system of their own. The cooling of V1 and H1 is conducted through $\diamond EDMN$

to the large block. The thermal distortion on the two knife edges is very small, about 10 microns for V1 in the worst case as shown in Fig. 2. Because of the thermal distortion component U_z of the large block, V1 will never have a surface area larger than 100 micron × 65 mm that is subjected to the x-ray beam. Suppose U_z is 80 microns for the large block, the surface area subjected to the x-ray beam will decrease to 20 microns × 65 mm, which will induce only a 1-micron thermal distortion.

Edge V1 remains perfectly flat even at the worst case; there is only a 1-2 micron difference between the center and the two sides of the knife edge as shown in Fig. 2. This is because the cooling tube is far away (at least 30 mm) from the heating surface; the temperature distribution is more even throughout the knife edge, so that the displacement component U_z along the knife edge is nearly constant. The relative displacement $\triangle_{2-1}$ (relative to point 1) is less than 1 micron as shown in Fig. 2.

5 Future Work

The idea of coating a low-Z material (for example, graphite) on the heating surface ($\Diamond ADEF$) of the large block was also evaluated in preliminary calcultions. If it becomes technically possible to braze 1-mm-thick graphite (k=12 $\frac{W}{cm\ ^{\circ}K}$) on tungsten or TZM, the thermal-structural results become very promising. The maximum temperature on the tungsten is calculated to be about 165°C. The maximum displacement component U_z is about 28 microns.

For each low-Z material element (in the finite element model), the absorbed power can be written as

$$q_{Absorb}(\frac{W}{Volume}) = \int_{E_{min}}^{E_{max}} S(E) \cdot exp^{-\alpha(E) \cdot x} \cdot \alpha(E) \cdot dE. \tag{7}$$

For high-Z materials, the transmitted power that hits on the surface of the tungsten (or TZM), after passing through the thickness of the low-Z material, can be written as:

$$q_{transmited}(\frac{W}{Area}) = \int_{E_{min}}^{E_{max}} S(E) \cdot exp^{-\alpha(E) \cdot x} \cdot dE, \tag{8}$$

where

S(E) =		source spectrum
$\alpha(E)$ =	$\frac{1}{thickness}$	absorption coefficient of low-Z material (function of material and energy)
z		thickness.

The program USP [6] was used to calculate the Undulator A spectrum, and the program TRANSMIT (part of SHADOW [7]) was used to calculate the function of $\alpha(E)$.

6 Acknowledgments

This work was supported by the U.S. Department of Energy, BES-Materials Science, under contract W-31-109-Eng-38. Editing by Susan Picologlou is appreciated.

References

[1] D. Shu, C. Brite, T. Nian, D. Haeffner, E. Alp, W. Yun, and T. M. Kuzay. Precision White Beam Slit (L5) Design for High Power Density X-ray Undulator Beamlines at the Advanced Photon Source, to be submitted to SRI 1994.

[2] B. Lai, A. Khounsary, R. Savoy, L. Moog, and E. Gluskin. Undulator A Characteristics and Specifications, Argonne National Laboratory, ANL/APS/TB-3, 1993.

[3] Tuncer M. Kuzay, A. M. Khounsary, and P. J. Viccaro. Enhanced Heat Transfer with metal Wool-Filled Tubes. Proc. ASME/JSME Thermal Engineering Joint Conference (Book No. 10309E-1991) 451-459.

[4] Mi-Tech Metals Inc. Indianapolis, Indiana 46218.

[5] H.L. Nian, I.C. Albert Sheng and Tuncer M. Kuzay. Thermal Analysis of a Photon Shutter for APS Front Ends, Nucl. Instr. and Meth. A319, 197 (1992).

[6] R. J. Dejus, Program USP.

[7] B. Lai and F. Cerrina. SHADOW: A Synchrotron Radiation Ray Tracing Program, Nucl. Instrum. and Methods. A 246, 337 (1986).

Figure Captions

Figure 1: Computer Model of the Final Design for L1 Vertical Slit

Figure 2: The Displacement (U_z) Contour of the Knife Edge Slit

Figure 3: Channel Model and Simplified Plate Model for Closed Form Solution

Figure 4: Parametric Study of the Maximum Temperature ($^\circ C$), Various h and Wall Thicknesses

Figure 5: Temperature Contour of the Large Block when the Maximum U_z occurs

Figure 6: The Displacement (U_z) Contour of the Large Block when the Maximum U_z Occurs

Figure 7: Temperature Contour of the Large Block when the X-ray Beam Hits Both $\diamond ADEF$ and $\diamond ABGH$

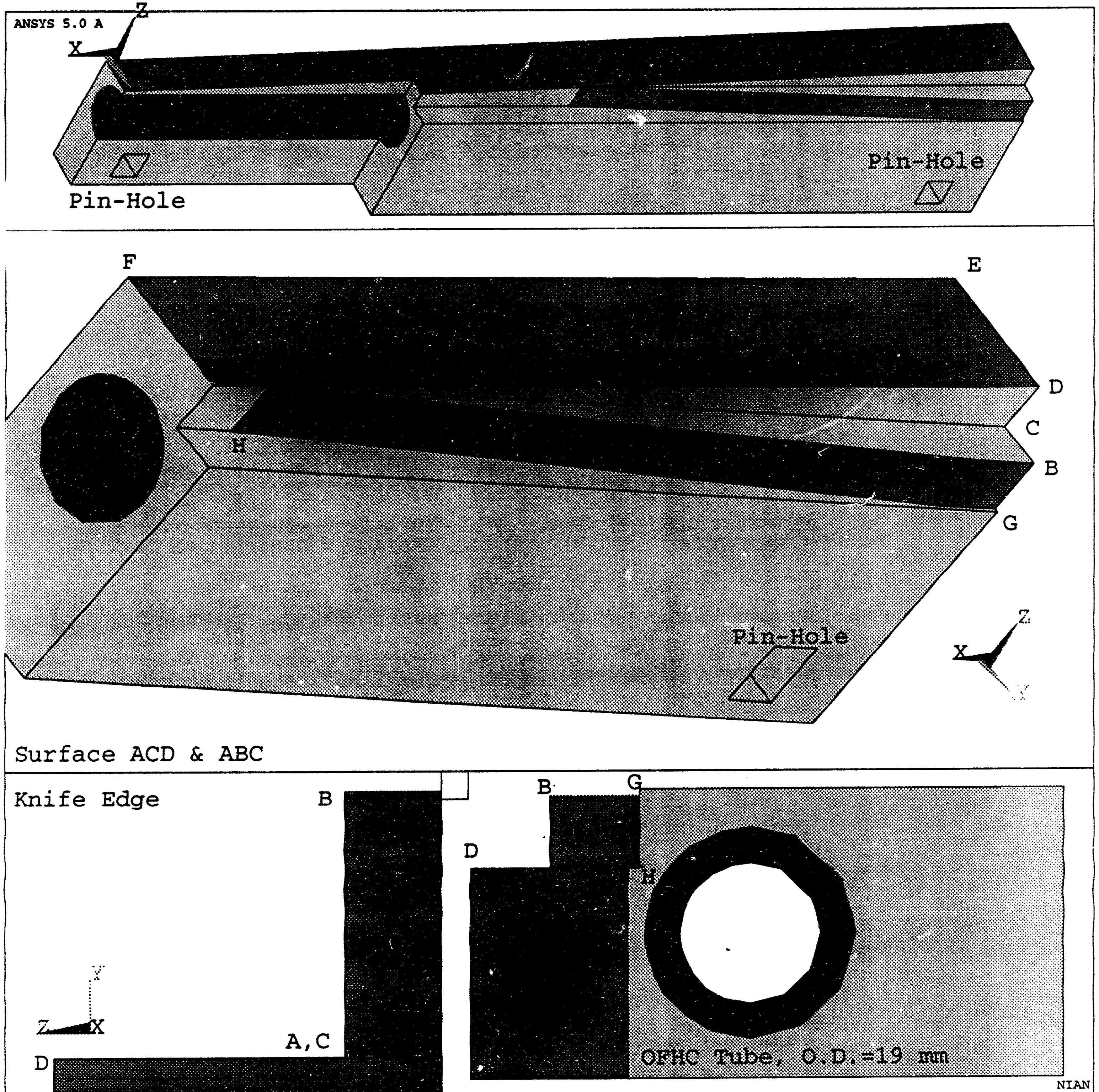
ANSYS 5.0 A
Z
X
Pin-Hole
Pin-Hole
F
E
D
C
H
B
G
Pin-Hole
Z
X
Surface ACD & ABC
Knife Edge
B
Y
Z
X
A,C
D
B
G
D
H
OFHC Tube, O.D.=19 mm
NIAN

Figure 1

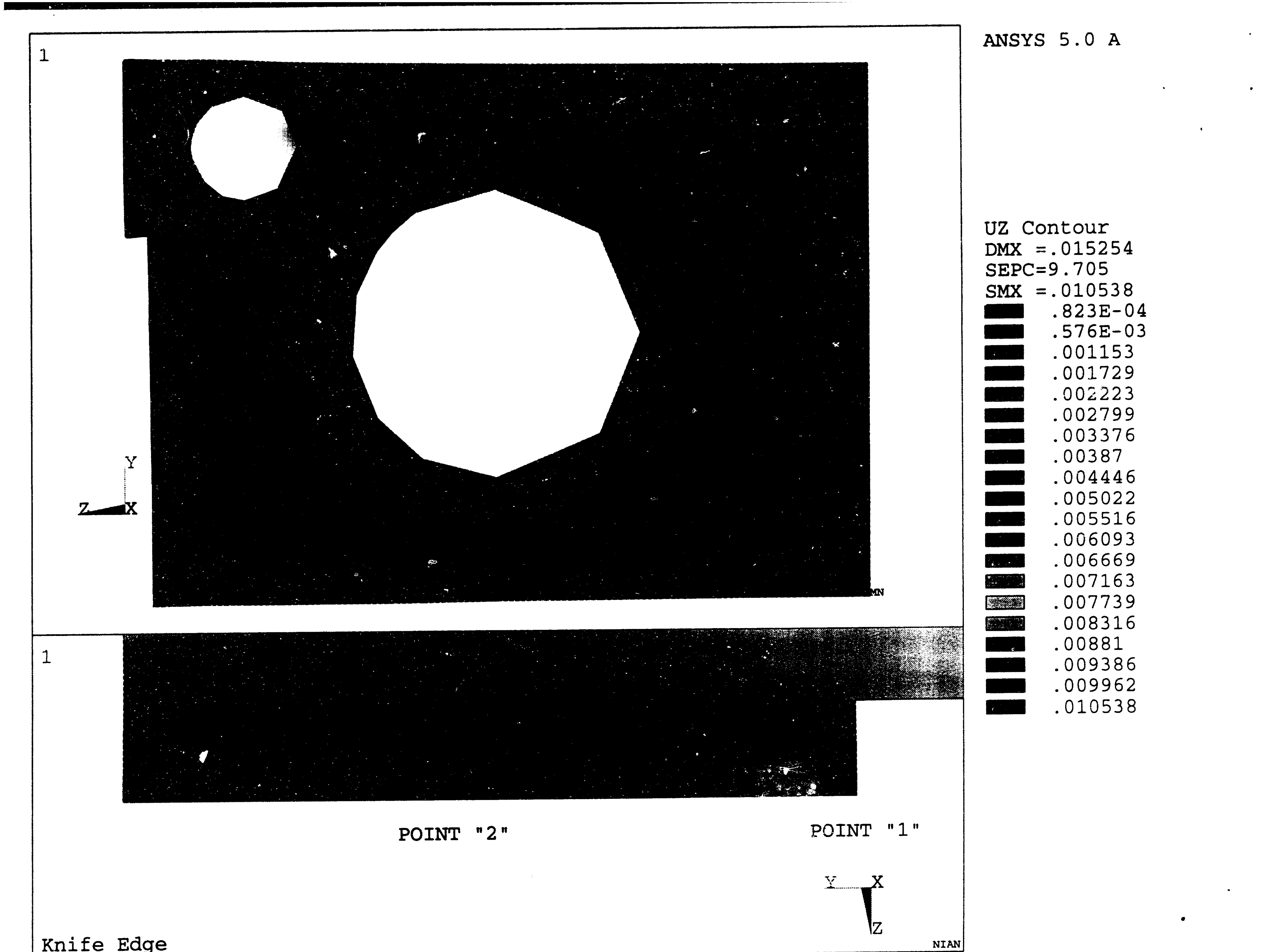

ANSYS 5.0 A
1
UZ Contour
DMX =.015254
SEPC=9.705
SMX =.010538
.823E-04
.576E-03
.001153
.001729
.002223
.002799
.003376
.00387
.004446
.005022
.005516
.006093
.006669
.007163
.007739
.008316
.00881
.009386
.009962
.010538
Y
Z
X
MN
1
POINT "2"
POINT "1"
Y
X
Z
Knife Edge
MX

Figure 2

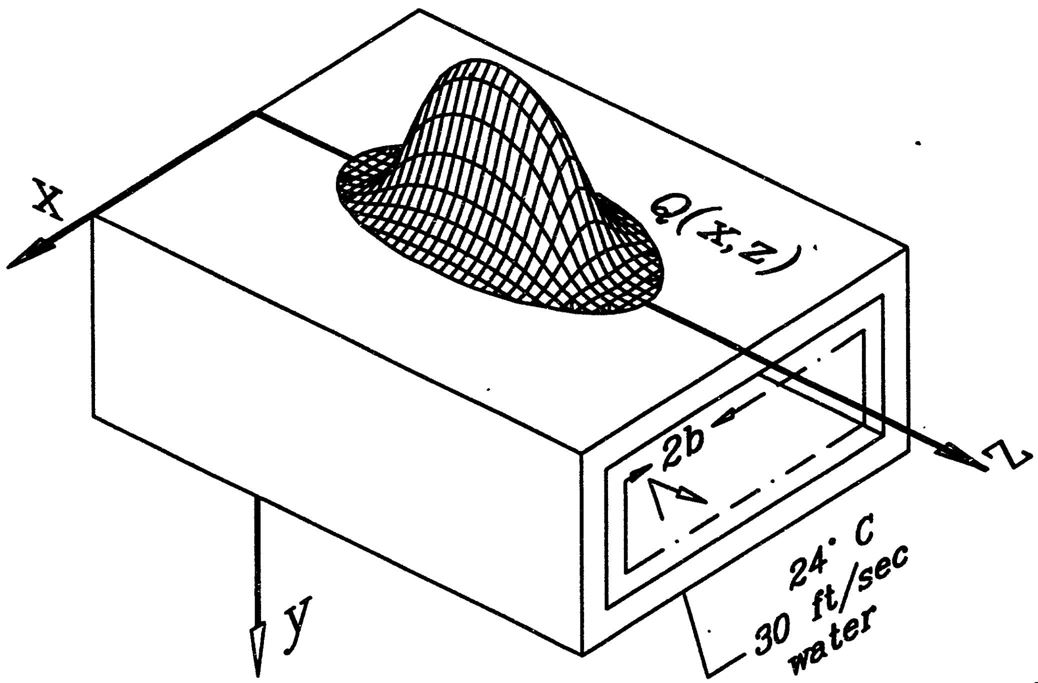

Channel Model with Real Beam Profile (ANSYS)

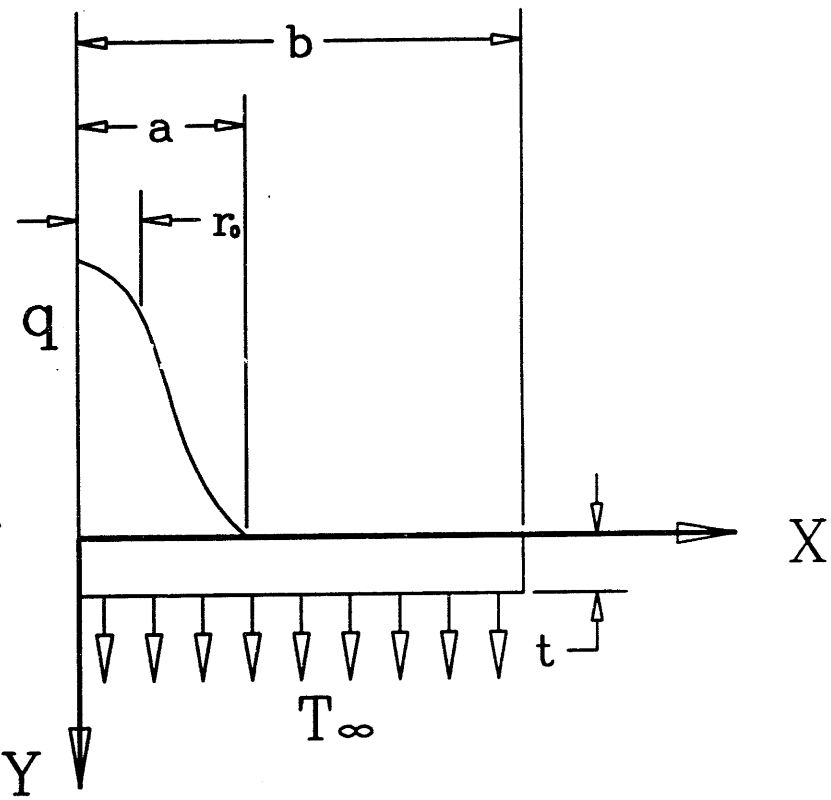

Simplified Model with Curve-Fit Gaussian Profile (Closed Form)

Fig. 8

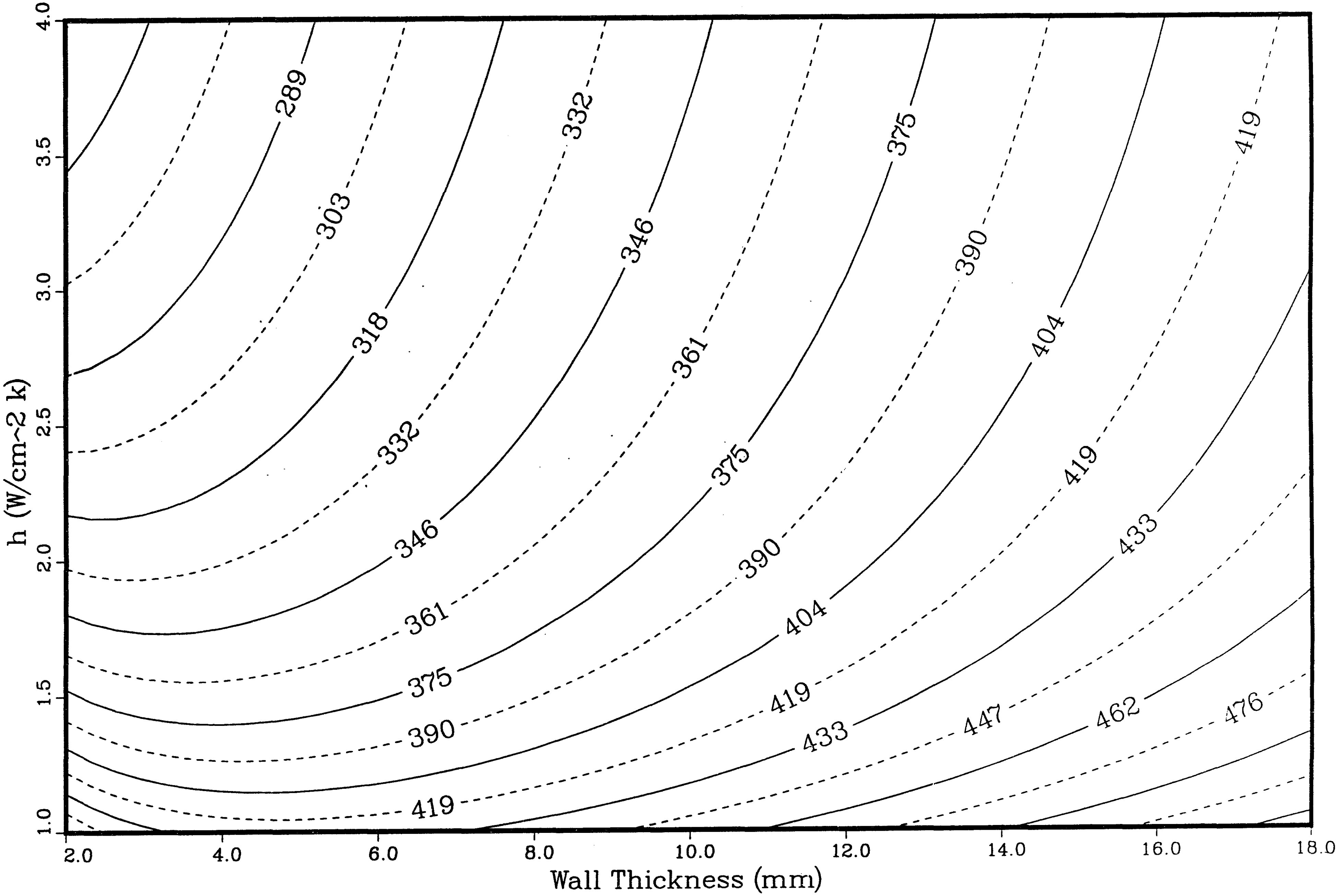

h (W/cm^2 k)
Wall Thickness (mm)
4.0
3.5
3.0
2.5
2.0
1.5
1.0
2.0
4.0
6.0
8.0
10.0
12.0
14.0
16.0
18.0
289
303
318
332
346
361
375
390
404
419
433
447
462
476

Fig. 4

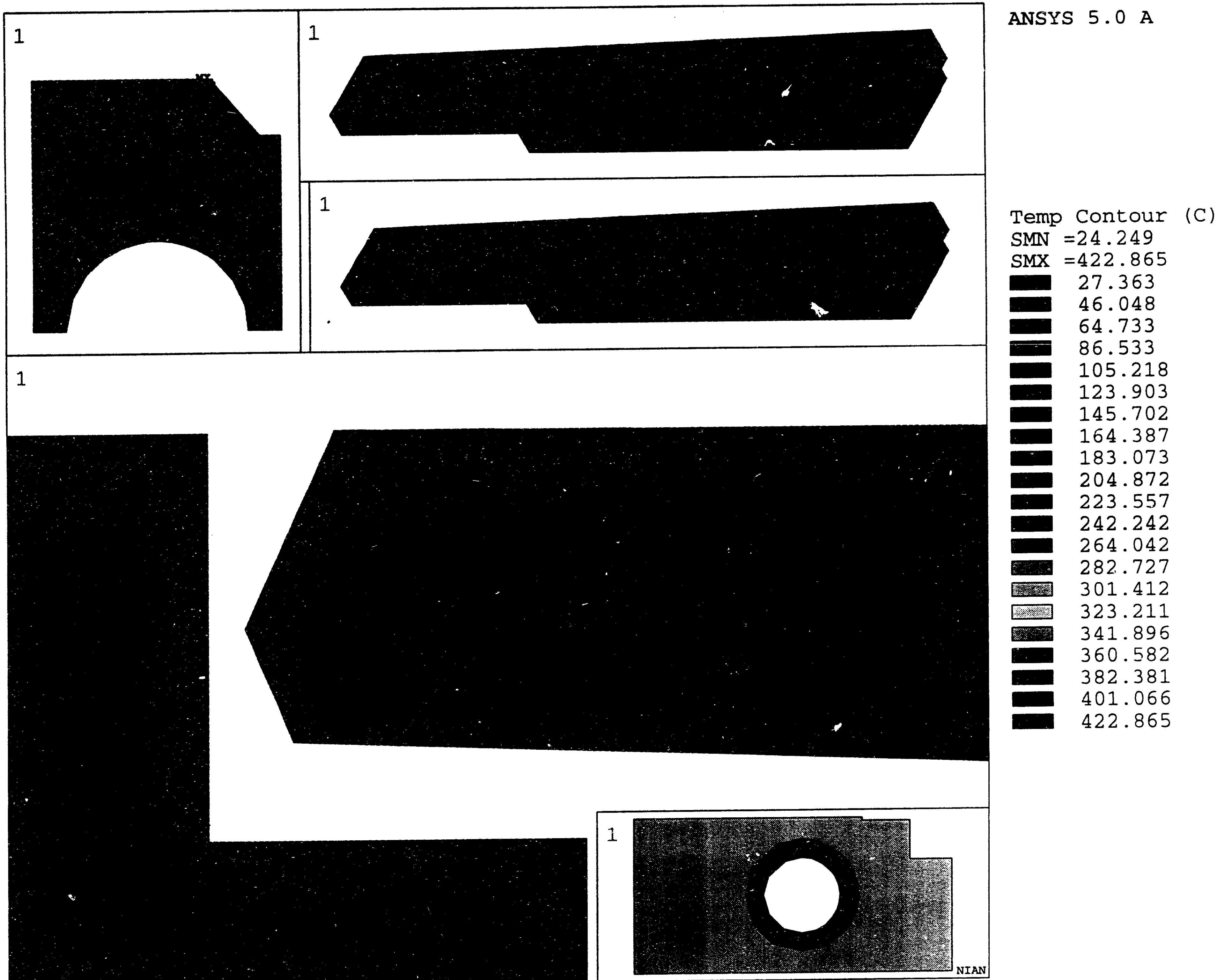
ANSYS 5.0 A
Temp Contour (C)
SMN =24.249
SMX =422.865
27.363
46.048
64.733
86.533
105.218
123.903
145.702
164.387
183.073
204.872
223.557
242.242
264.042
282.727
301.412
323.211
341.896
360.582
382.381
401.066
422.865
1
1
1
1
1
NIAN

Figure 5

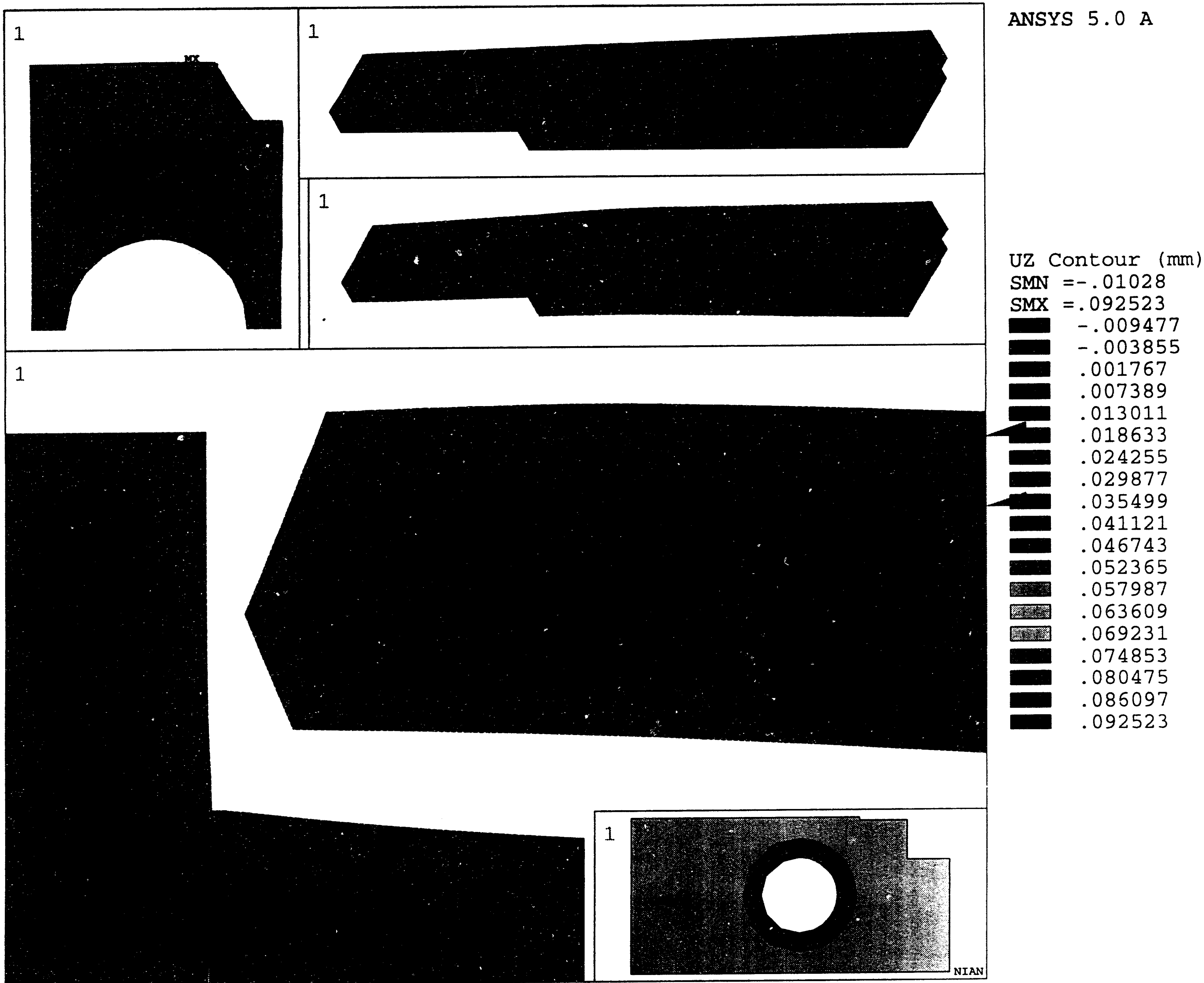

ANSYS 5.0 A
1
MX
1
1
1
1
NIAN
UZ Contour (mm)
SMN =-.01028
SMX =.092523
-.009477
-.003855
.001767
.007389
.013011
.018633
.024255
.029877
.035499
.041121
.046743
.052365
.057987
.063609
.069231
.074853
.080475
.086097
.092523

Figure 6

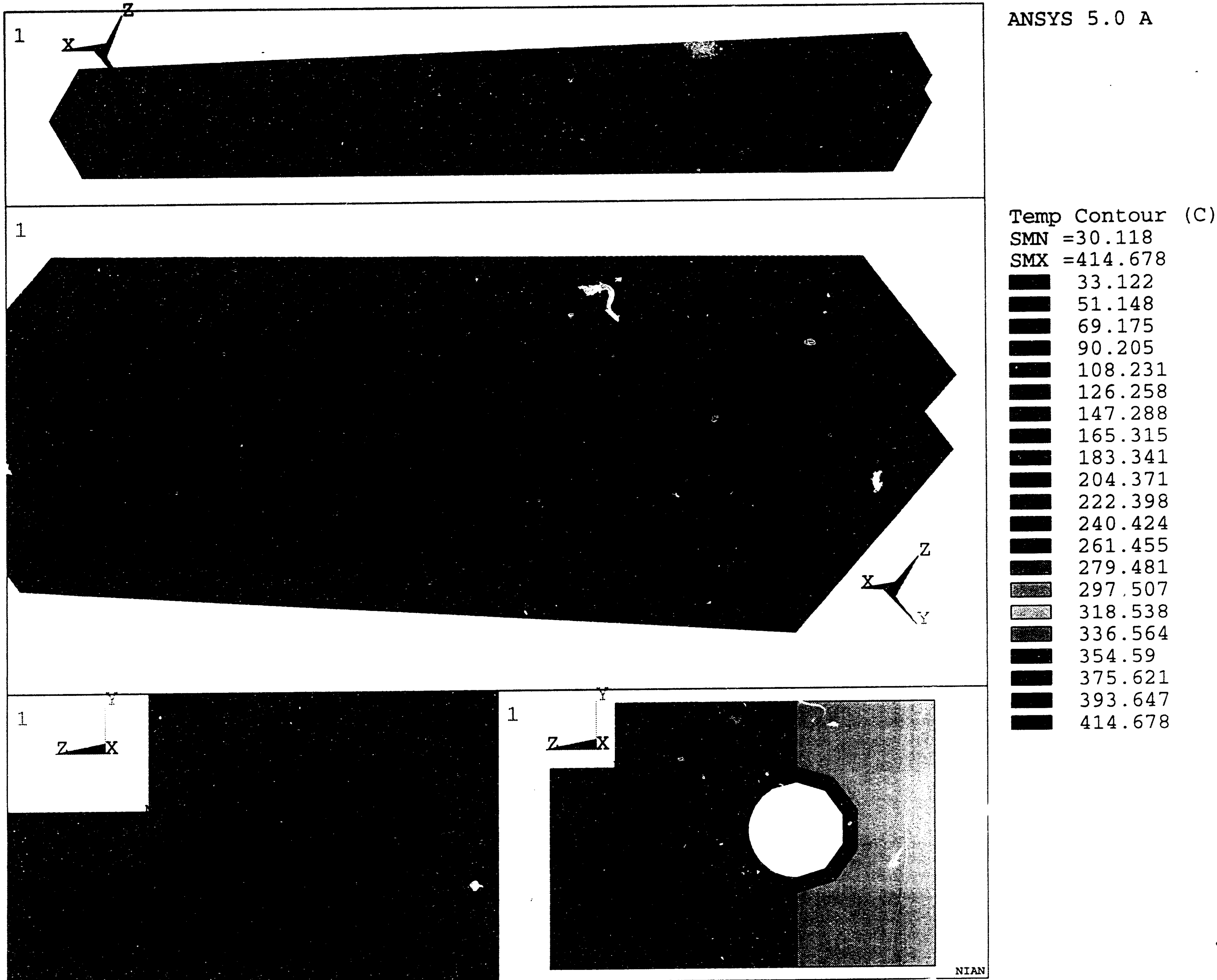

ANSYS 5.0 A
1
X
Z
1
X
Y
Z
1
Y
Z
X
1
Y
Z
X
Temp Contour (C)
SMN =30.118
SMX =414.678
33.122
51.148
69.175
90.205
108.231
126.258
147.288
165.315
183.341
204.371
222.398
240.424
261.455
279.481
297.507
318.538
336.564
354.59
375.621
393.647
414.678
NIAN

Figure 7

DATE
FILMED
10/14/94

END